

1 **Instantaneous stomatal optimization results in suboptimal carbon gain due to legacy effects**

2 Xue Feng^{1,2}, Yaojie Lu¹, Mingkai Jiang³, Gabriel Katul⁴, Stefano Manzoni⁵, Assaad Mrad^{6,7}, Giulia Vico⁸

3

4 ¹Department of Civil, Environmental, and Geo-Engineering, University of Minnesota, Minneapolis, MN

5 55455, USA;

6 ²Saint Anthony Falls Laboratory, University of Minnesota, Minneapolis, MN 55455, USA

7 ³Hawkesbury Institute for the Environment, Western Sydney University, Locked Bag 1797, Penrith 2751,

8 NSW, Australia.

9 ⁴Department of Civil and Environmental Engineering, Duke University, Durham, NC 27708, USA;

10 ⁵Department of Physical Geography and Bolin Centre for Climate Research, Stockholm University,

11 Stockholm, Sweden

12 ⁶Department of Civil & Environmental Engineering, University of California Irvine, CA 92695, USA

13 ⁷Department of Engineering, Wake Forest University, NC 27101, USA

14 ⁸Department of Crop Production Ecology, Swedish University of Agricultural Sciences (SLU), 750 07

15 Uppsala, Sweden

16 **Corresponding authors:**

17 Xue Feng: <https://orcid.org/0000-0003-1381-3118>; feng@umn.edu

18 Yaojie Lu: <https://orcid.org/0000-0002-5215-6109>; tanisraistlin@gmail.com

19

20 **ABSTRACT**

21 Stomatal optimization has been a common phenomenological approach to represent plant stomatal
22 regulation for decades. Recent studies that maximize the instantaneous net carbon gain reproduce
23 empirical stomatal conductance variations in relation to fast environmental stimuli such as
24 photosynthetically active radiation and vapor pressure deficit. However, this instantaneous stomatal
25 optimization framework lacks the ability to account for 'legacy effects' associated with plant-
26 environment feedbacks. Here, the solutions of two stomatal optimization models that do and do not
27 account for these legacy effects are compared. The comparisons focus on stomatal conductance,
28 transpiration rates, net carbon gain rates, and permanent xylem damage over time under different
29 rainfall regimes and in the presence and absence of competition. It is shown that the optimal solution
30 resulting from the instantaneous stomatal optimization is significantly less productive in most scenarios
31 and not viable when xylem embolism cannot be fully repaired. Accounting for legacy effects improves
32 plant productivity and therefore is essential to understanding stomatal regulation based on the
33 optimality principle. These model comparisons demonstrate that legacy effects are significant to shape
34 vegetation acclimation and adaptation responses to climate and environmental change, and thus must
35 be resolved in future stomatal optimization schemes.

36 **Key words:** instantaneous carbon maximization, legacy effect, permanent xylem embolism, stochastic
37 rainfall, stomatal optimization, water competition

38

39 **1. INTRODUCTION**

40 Stomatal regulation is a cornerstone process that links the exchange of carbon and water between
41 vegetation and atmosphere and how it is affected by plant water stress. Its significance to plant
42 physiology and evolution is not in dispute and has motivated centuries of research (Hetherington &
43 Woodward, 2003). Stomatal regulation has also been recognized for its key role in global environmental
44 change, by coupling the terrestrial water, carbon, and energy cycles at the ecosystem level (Gentine *et*
45 *al.*, 2019) and defining the risk of plant vulnerability to and mortality from drought (Martin-StPaul *et al.*,
46 2017; Anderegg *et al.*, 2018; Hochberg *et al.*, 2018; Blackman *et al.*, 2019; Feng *et al.*, 2019).

47 An important contribution to the understanding of stomatal regulation is the theory of stomatal
48 optimization, which was first proposed by Cowan & Troughton (1971) and later expanded upon by
49 Cowan & Farquhar (1977) and many others (Buckley *et al.*, 2017; Harrison *et al.*, 2021). In the process of
50 gaseous CO₂ uptake, water vapor molecules are inevitably lost through the stomata and must be
51 replenished from the soil reservoir. Inspired by this observation, Cowan & Troughton (1971), Givnish &
52 Vermeij (1976), Cowan & Farquhar, (1977), and Hari *et al.* (1986) cast stomatal regulation as an
53 economic problem of leaf-level plant gas exchange: plants, constrained by a fixed water supply in the
54 soil, regulate stomatal conductance in response to environmental cues to achieve maximum carbon gain
55 over a prescribed time period (presumed to be much longer than the timescale at which guard cells
56 open or close). Under certain restricted conditions (usually when the resource constraint is not severe),
57 the solutions based on stomatal optimization provide a means to predict how stomatal conductance
58 varies with environmental cues (e.g., vapor pressure deficit, light, CO₂ concentration, and to a lesser
59 extent soil moisture availability). Since then, various ‘off-shoots’ and modifications to this optimization
60 framework have emerged, with different goals (e.g., minimize water loss; Sperry & Love, 2015; Sperry *et*
61 *al.*, 2017) and constraints (e.g., water limitation is prescribed instantaneously through “profit
62 maximization”, Wolf *et al.*, 2016) associated with stomatal regulation. Stomatal optimization has since
63 then complemented empirical (e.g., Jarvis, 1976; Ball *et al.*, 1987; Leuning, 1995) and mechanistic
64 models (e.g., Hills *et al.*, 2012) as a top-down, goal-oriented approach to study stomatal regulation.
65 Some of these solutions have been incorporated into vegetation productivity (e.g., Stocker *et al.*, 2020)
66 and land surface models (e.g., Medlyn *et al.*, 2011; Eller *et al.*, 2020). In short, stomatal optimization
67 theory is at the basis of several recent formulations and is increasingly adopted into a wide range of
68 models. There is also unprecedented opportunity to evaluate their predictions from in situ
69 measurements, observation networks, and remote sensing products. The time is thus ripe to revisit the

70 premises of the stomatal optimization theory and how they relate to fundamental conceptualizations of
71 plant water use, for a better-informed application of this phenomenological approach.

72 The goal at the heart of stomatal optimization is the maximization of cumulative carbon gain over some
73 period as a proxy of ecological fitness and reproductive success. Yet, plants' current water use affects
74 their future carbon gain, by using resources now that would then not be available in the future or
75 incurring in damage that would jeopardize future carbon gains – which we label as “legacy effects”. In
76 fact, this temporal tradeoff between current water use and future carbon gain is implicit in Cowan and
77 Farquhar's original formulations of the stomatal optimization problem: how can plants optimally
78 distribute a *fixed* amount of water over a specified period of time? Because cumulative carbon gain is
79 the result of continuous investment of carbon and other resources by plants over time, legacy effects
80 decouple the optimal strategy from instantaneous environmental cues. That is, maximizing
81 instantaneous carbon gain would trivially result in maximum stomatal conductance until soil water is
82 completely depleted. To achieve more realistic predictions through instantaneous optimization (and to
83 bypass issues related to the interpretation of the Lagrange multiplier-parameter in Cowan and
84 Farquhar's formulation), various cost functions related to transpirations rates or plant water potential
85 have been introduced (as reviewed in Wang *et al.*, 2020). How these cost functions can, at a single point
86 in time, approximate the time-integrated legacy effects remains an open question (Buckley &
87 Schymanski, 2014).

88 The central question concerning the role of legacy effects is this: can plants maximize their cumulative
89 net carbon gain over time by maximizing their net carbon gain at every single moment? We hypothesize
90 that this is not the case because legacy effects will incur opportunity costs on plants' current water use
91 in the form of reduced future carbon gain. A strategy that maximizes net carbon gain at every moment,
92 in the presence of legacy effects, will inevitably reduce the highest possible net carbon gain in the future
93 and thus the cumulative net carbon gain over time.

94 Here we test this hypothesis by comparing the optimal stomatal strategies that account for legacy
95 effects against representative stomatal optimization models developed in recent years that do not
96 account for legacy effects. Especially, we consider their ability to account for legacy effects associated
97 with plant-environment feedback and co-evolution and how these legacy effects affect plant
98 performance under varying drought conditions. We anticipate these legacy effects to play an important
99 role in shaping vegetation acclimation and adaptation responses to climate and environmental change.

100 **2. THEORY**

101 **2.1. Legacy effects**

102 Amongst the many possible types of legacy effects, previous studies have explored the role of soil-plant
103 feedback and permanent or irrecoverable xylem embolism. The first type, the soil-plant feedback, is a
104 temporal tradeoff between plants' current water consumption and their future soil water availability
105 (Manzoni *et al.*, 2013; Mrad *et al.*, 2019). Amongst all the environmental cues relevant to plant gas
106 exchange, soil water stands out as the only one strongly regulated by plants themselves. That is, the
107 more water plants consume now, the less water will be left for them in the future during a single dry-
108 down (Cowan & Farquhar, 1977; Cowan, 1986). In contrast, other environmental variables can
109 effectively be considered to be external conditions – i.e., be independent of plant influence – at the
110 intermediate timescale of drought-induced water stress, although plants do have the ability to partially
111 regulate vapor pressure deficit or CO₂ concentrations in the atmosphere at multiple time scales
112 spanning boundary layer dynamics to multi-decadal (Lebrija-Trejos *et al.*, 2010). At low soil moisture
113 levels, plants may be forced to give up CO₂ uptake partially or completely due to the elevated risk of
114 desiccation. It follows that any optimal behavior by plants should account for the fact that the increase
115 in current carbon gain due to increased water consumption comes at the cost of reduced future carbon
116 gain due to decreased water availability. Under certain conditions, the plant's ability to partially adjust
117 atmospheric vapor pressure deficit and air temperature can impact predisposition to rainfall (Siqueira *et*
118 *al.*, 2009; Konings *et al.*, 2010), but this effect will not be explicitly considered here.

119 The second type of legacy effect is permanent or irrecoverable xylem embolism. Xylem embolism is
120 incurred when the growing mismatch between water supply and demand reduces the plant's capacity
121 for xylem water transport. If not fully repaired, an embolized xylem will limit the water supply from the
122 soil to the leaves (even if soil water becomes abundant again). In turn, this will potentially induce
123 stomatal closure that reduces CO₂ uptake for photosynthesis (Hubbard *et al.*, 2001; Sperry *et al.*, 2002;
124 Anderegg *et al.*, 2014). Thus, this effect of permanent xylem embolism can also be regarded as an
125 opportunity cost of reduced future carbon gain (Wolf *et al.*, 2016). In the extreme case of hydraulic
126 failure, plants are forced to stop photosynthesis completely. Therefore, permanent xylem damage
127 complicates stomatal optimization by introducing a tradeoff between plants' current water use and their
128 future water transport capacity. Similar arguments can be extended to the phloem system, though the
129 focus here is maintained on the xylem for illustration purposes (Konrad *et al.*, 2018).

130 **2.2. The “Dynamic-Feedback” Approach**

131 Relevant to the consideration of legacy effects, recent advances in stomatal optimization can be
132 grouped into two broad categories (Table 1): (i) an “instantaneous” approach that achieves maximum
133 net carbon gain based on given environmental inputs at every instant, and (ii) a time-explicit, “dynamic
134 feedback” approach that optimizes stomatal conductance over time to maximize *cumulative* carbon
135 gain. Both approaches can respond to changing environmental conditions. The key difference is that the
136 instantaneous approach determines the optimal stomatal conductance based on the current
137 information only, including current environmental conditions and plant water status (e.g., xylem
138 hydraulic damage), whereas the dynamical feedback approach characterizes the optimal stomatal
139 conductance behavior based on current and future information. Here, the difference between
140 instantaneous and dynamic-feedback approaches should be distinguished from the idea that plants may
141 encode past information through genetic memory resulting from natural selection (e.g., functional traits
142 that characterize xylem vulnerability curves). That is, plants may adapt to past and future environmental
143 conditions through functional traits that define their water use strategies, but these traits are treated as
144 being static within both instantaneous and dynamic-feedback approaches. Therefore, it is reasonable to
145 expect instantaneous approaches to account for past information through parameterized traits, but this
146 type of past information can be similarly accounted for by dynamic-feedback approaches. In contrast,
147 the defining difference between instantaneous and dynamic-feedback approaches lies in their ability to
148 account for the implications on future resource availability or acquisition (i.e., legacy effects) in the
149 process of finding the optimal behavior.

150 In practice, the instantaneous optimization approach has shown an extraordinary capacity to reproduce
151 empirical patterns (Sperry *et al.*, 2017a; Venturas *et al.*, 2018; Bassiouni & Vico, 2021), especially in
152 relation to high frequency (e.g., diurnal) vapor pressure deficit responses (Katul *et al.*, 2009, 2010).
153 However, the fundamental premise of the instantaneous approach is that plants should trade as much
154 future carbon gain as possible for the current carbon gain. This tradeoff does not always make sense as
155 plants undergo soil water stress over time, as plant water-use efficiency (WUE) increases with moderate
156 soil water stress (DeLucia & Heckathorn, 1989) and thus water (on a per carbon basis) becomes less
157 costly.

159 **Table 1:** Examples of instantaneous and dynamic-feedback stomatal optimization models, including
 160 optimization methodology and the definitions for their objective functions, costs θ , and constraints. ESS
 161 refers to the evolutionarily stable strategy under competitive environments.

Models	Optimization approach	Objective function	Cost function, θ	Legacy effects considered (Feedback constraints)
Instantaneous				
<i>Prentice et al. (2014)</i>	Instantaneous	$\min \theta$	$\frac{jE}{A} + \frac{mV_{c,max}}{A}$	None
<i>Wolf et al. (2016)</i>	Instantaneous, ESS	$\max(A - \theta)$	$uP^2 + vP + w$	None
<i>Sperry et al. (2017)</i>	Instantaneous, ESS	$\max(A - \theta)$	$A_{max} \left(1 - \frac{k}{k_{max}}\right)$	None
<i>Eller et al. (2018)</i>	Instantaneous, ESS	$\max(A - \theta)$	$A \left(1 - \frac{k}{k_{max}}\right)$	None
Dynamic feedback within a single dry down				
<i>Cowan & Farquhar (1977)</i>	Dynamic feedback	$\max \int_0^T A \, dt$	None	$\int_0^\infty E \, dt \leq W_0, \frac{dW}{dt} = -E$
<i>Mäkelä et al. (1996)</i>	Dynamic feedback	$\max \int_0^\infty e^{-\lambda t} A \, dt$	None	$\int_0^\infty E \, dt \leq W_0, \frac{dW}{dt} = -E$ (rainfall is stochastic)
<i>Manzoni et al. (2013)</i>	Dynamic feedback	$\max \int_0^T A \, dt + J_T$	None	$\frac{dW}{dt} = -(E + L)$
<i>Mrad et al. (2019)</i>	Dynamic feedback	$\max \int_0^T A \, dt + J_T$	None	$\frac{dW}{dt} = -(E + L)$ (E also specified by plant hydraulics)
Dynamic feedback over consecutive dry downs				
<i>Lu et al. (2016)</i>	Dynamic feedback	$\max \int_0^\infty \bar{A} \, dt$	None	$\frac{dW}{dt} = R - E - L$ (rainfall R is stochastic)
<i>Lu et al. (2020)</i>	Dynamic feedback, ESS	$\max \int_0^\infty \overline{A - \Theta} \, dt$	$\beta \left(1 - \frac{k}{k_{max}}\right)$	$\frac{dW}{dt} = R - E - L$ (rainfall R is stochastic) Permanent xylem embolism

162 *Abbreviations.* A : net photosynthetic rate, T : dry down duration, λ : rainfall frequency per day, P :
 163 absolute value of leaf xylem pressure, J_T : carbon value of terminal soil moisture, $V_{c,max}$: maximum
 164 carboxylation rate, j, m, u, v, w : fitting parameters, k : soil-plant hydraulic conductance, k_{max} : maximum
 165 hydraulic conductance with no transpiration or no xylem cavitation, β : carbon cost per unit of recovered
 166 k , W : soil water storage in the rooting zone, W_0 : soil water available at beginning of dry down, R : rainfall,
 167 E : evapotranspiration, L : leakage below the rooting zone. Overbar on \bar{A} and $\overline{A - \Theta}$ indicates temporal
 168 averages due to random nature of rainfall.

169 The dynamic feedback approach incorporates an explicit time component into the description of the
170 optimal trajectory of stomatal aperture. This addition provides a feedback related to temporal tradeoffs
171 in water use and carbon uptake. The temporal characterization provides a necessary (but not sufficient)
172 basis to account for legacy effects – not only of soil-water feedback and permanent xylem embolism,
173 but also of others related to plant physiology and conservation of resources. In the last decade, it has
174 become increasingly clear that leaf-level gas exchange is closely connected with many other plant
175 physiological processes and thus should not be autonomously optimized. For example, efforts have been
176 made to couple plant hydraulic and sucrose transport constraints (Huang *et al.*, 2018), soil salinity (Perri
177 *et al.*, 2019), leaf phenology (Konrad *et al.*, 2017), belowground allocation (Schymanski *et al.*, 2009), and
178 soil-to-leaf nutrient regulation (Buckley *et al.*, 2002; Palmroth *et al.*, 2013) into stomatal optimization, all
179 of which effectively reformulate the original stomatal optimization problem from leaf-level to whole-
180 plant level (Buckley, 2021).

181 Finally, recent work has also expanded on the idea that stomatal regulation can be formulated as either
182 a carbon maximizing, ecological strategy problem (e.g., Cowan & Farquhar, 1977) or a competition-
183 driven, evolutionary strategy problem (e.g., Wolf *et al.*, 2016) (Table 1). These alternative formulations
184 diverge fundamentally in the conceptualization of an “optimal” solution, requiring different
185 mathematical tools. The carbon maximization paradigm maximizes the carbon gain of individual plants,
186 and its solutions are derived using optimal control theory (e.g., Mäkelä *et al.*, 1996). Soil evaporation
187 and drainage are seen as processes “competing” with plants for soil water, reducing the benefit of
188 leaving water for later use and thus affecting the optimal stomatal response (Cowan 1982). In contrast,
189 the competition paradigm stems from game theory and searches for an evolutionarily stable strategy
190 (ESS, Maynard Smith, 1974) for stomatal response to environmental cues, with which plants can
191 guarantee a higher or equal carbon gain against competitors with any alternative stomatal strategy
192 when competing for water (i.e., when neighboring plants share access to a local soil water pool). Both
193 paradigms are theoretically sound, and both can be formulated in a time-explicit or an instantaneous
194 manner, but caution should be used when comparing their predictions given their differing premises for
195 stomatal optimization. In practice, the presence of competition has often been used as justification for
196 neglecting temporal effects through the instantaneous approach (Wolf *et al.* 2016). However, the
197 compensatory effect of competition is never absolute. Even for plants subject to competition, some of
198 the water saved by a more conservative water use strategy can be used later by the same plant. In
199 addition, excessive water use may impair plants’ future ability to take up water in a way that has no

200 influence on a competitor's current water uptake ability. Thus, it is possible to subject plants
201 simultaneously to competition as well as time explicit legacy effects (Lu *et al.*, 2020).

202 The conjecture to be explored here is that the time-explicit, dynamic feedback approach is more
203 appropriate (i.e., results in higher cumulative carbon gain) in the presence of legacy effects than the
204 instantaneous approach. To this end, we compare calculations from the dynamic feedback approach
205 against the instantaneous approach. In this comparison, we consider the two types of legacy effects (i.e.,
206 soil-plant feedback and permanent xylem damage) and two 'end-member' timescales of soil moisture
207 variability: (i) during a single dry-down (no precipitation, so that water availability is dictated by the
208 initial root-zone soil moisture content), and (ii) stochastic rainfall (equivalent to a sequence of
209 consecutive dry-downs after random rainfall inputs). We demonstrate that by accounting for these
210 legacy effects, the optimal solution from the dynamic feedback approach results in greater cumulative
211 net carbon gain for plants than that based on the instantaneous carbon gain rate.

212 **3. METHODS**

213 We directly compare the instantaneous and dynamic feedback stomatal optimization strategies. These
214 two strategies are derived under the same modeling conditions (see the *Plant gas exchange model*
215 section), including the legacy effects of soil-plant feedback and permanent xylem embolism (see Table
216 S1), but under different optimization goals (see the *Optimization goals* section), resulting in different
217 quantitative responses of stomatal conductance to environmental conditions. To illustrate their
218 differences, we compare them in two dry-down scenarios (i.e., the single dry-down and stochastic
219 rainfall scenarios), which are defined in the *Dry-down scenarios* section. Soil water availability is treated
220 as the only dynamic resource, while all the other environmental cues (e.g., vapor pressure deficit) are
221 externally supplied (as constants for ease of comparisons). All the symbols and their definitions are
222 given in Table 2.

223 **3.1. Plant gas exchange model**

224 To allow for a direct comparison, we use the same model to calculate the dynamic feedback and
225 instantaneous optimal stomatal strategies following the setup from Eller *et al.* (2018). The associated
226 parameter values are also kept the same (see Table 1 in Eller *et al.*, 2018). The model by Eller *et al.*
227 (2018) describes how plant photosynthesis and transpiration rates depend on stomatal conductance.
228 Transpiration rate are also regulated by xylem hydraulic conductance and depend on plant hydraulic

229 traits as well as soil and plant water potentials. Finally, following Wolf *et al.* (2016), we assume the
230 existence of an instantaneous carbon cost of plant water use and define its dependence on
231 instantaneous plant water potential. In Table S1, we summarize the model equations and the references
232 in the original paper.

233 The model by Eller *et al.* (2018) does not have a component of permanent xylem embolism, so we use
234 the definition given by Lu *et al.* (2020) for both the instantaneous and dynamic feedback optimal
235 stomatal strategies. Briefly, permanent embolism changes the vulnerability curve of the xylem over
236 time. The extent to which xylem embolism can recover after embolism is defined as a prescribed
237 percentage, p_k , of the recovered vs unimpaired xylem conductance at a given water potential. Recovery
238 is assumed to take place instantaneously as soon as rewetting occurs. A p_k of 100% corresponds to
239 perfectly recoverable embolisms and indicates that the xylem vulnerability curve does not change with
240 successive embolisms. In contrast, a p_k of 0% corresponds to zero recovery, so plant hydraulic
241 conductance at any given time is determined by the lowest plant water potential yet experienced by the
242 plant up to that time. For intermediate cases ($0\% < p_k < 100\%$), the percentage loss of hydraulic
243 conductivity (PLC) is repaired only to a fraction p_k of the original, unimpaired xylem conductance at any
244 given water potential. Any percentage loss represented by $p_k < 100\%$ represents a legacy effect (the
245 lower the p_k , the larger the legacy effect) that irreversibly reduces plant hydraulic capacity as the soil
246 becomes progressively drier. More details on this scheme can be found in Lu *et al.* (2020) (e.g., Fig. 1,
247 Eqs. 4 & 5).

248 **3.2. Optimization goals**

249 There are two basic differences between the instantaneous and dynamic feedback stomatal
250 optimization strategies. First, instantaneous stomatal optimization strategies are presumed to be able to
251 competitively exclude all others (Wolf *et al.*, 2016), while different dynamic feedback stomatal
252 optimization strategies can be constructed in ways that do or do not account for competition for water
253 (Lu *et al.*, 2016, 2020) (Table 1). To compare these approaches, the performance of the same
254 instantaneous stomatal optimization strategy are examined and compared with the corresponding
255 dynamic feedback strategies, both in the absence or presence of competition for water, using the same
256 net carbon gain function.

257 Second, the instantaneous stomatal optimization strategy optimizes the instantaneous value of stomatal
258 conductance, g_s , given all atmospheric and soil moisture variables as external conditions. Conceptually,
259 this means that atmospheric or soil moisture conditions are not treated as internal variables, and their
260 temporal dynamics are not factored into the optimal stomatal strategy (which exerts “open loop
261 control”). In contrast, the dynamic feedback strategy optimizes the stomatal conductance including its
262 response to soil water availability, i.e., $g_s(s)$, where s represents the relative soil water content or degree
263 of saturation. Thus, the dynamic feedback strategy optimization results in a functional relation to soil
264 moisture, with only the atmospheric variables acting as external input. This is how the dynamic feedback
265 strategy can account for the ability of plants to dynamically regulate their own soil water supply (i.e., the
266 local soil moisture dynamics) and thus the legacy effect of soil-plant feedback (a “closed loop control”
267 with respect to soil water). It is possible to extend both approaches to include interactive effects
268 between plants and their micrometeorological states (Katul *et al.*, 2012; Manoli *et al.*, 2016), but this
269 extension is not considered here.

270 The instantaneous stomatal optimization strategy maximizes the instantaneous net carbon gain by
271 adjusting g_s , given the current atmospheric and soil conditions

$$\max_{g_s} B(g_s, s) \quad (1)$$

272 where B is the instantaneous net carbon gain rate (see Table S1 or Eqs. 2.8 & 2.9 in Eller *et al.* (2018)).
273 Note that B is typically expressed as the difference between carbon assimilation A and a cost function θ ,
274 which can be related to transpiration or decline in water potential (see Table 1 for a selection of
275 different cost functions). For convenience, we only show explicitly the dependence of B on s (i.e.,
276 relative soil water content, which is a state variable that ranges between 0 and 1) and g_s (the control
277 variable), but not on the atmospheric forcings (e.g., vapor pressure deficit, light) or static parameters
278 (e.g., photosynthetic capacity, hydraulic traits). The effect of g_s on whole-plant net carbon gain rate is
279 derived assuming a constant leaf area and well-coupled conditions between the plant and atmosphere
280 so that air temperature reasonably approximates surface temperature. These approximations are
281 imposed on both model formulations for the purposes of their comparison.

282 In the absence of competition for water, the dynamic feedback stomatal optimization strategy
283 maximizes the long-term average net carbon gain rate (equivalent to cumulative carbon gain) over a
284 specified time horizon by adjusting $g_s(s)$. Then, the corresponding objective function is

$$\max_{g_s(s)} \bar{B}(g_s(s), s) \quad (2)$$

285 where $\bar{B}(g_s(s), s)$ is the long-term average net carbon gain rate given the stomatal response to relative
 286 soil water availability $g_s(s)$,

$$\bar{B}(g_s(s), s) = \frac{1}{T} \int_0^T B(g_s(s(t)), s(t)) dt \quad (3)$$

287 where T marks the end of the optimization period. For example, in a simple single dry-down scenario, T
 288 is the prescribed length of the dry-down.

289 The maximization in Eq. 2 is subject to the water availability constraint – the cumulative transpiration at
 290 any given time cannot exceed the cumulative water supply, for any time τ from 0 to T . Mathematically,
 291 this constraint abides by

$$\int_0^\tau E(g_s(s(t))) dt \leq W(\tau), \forall \tau \in [0, T], \quad (4)$$

292 where $W(\tau)$ is the cumulative water supply up until time τ . In the case of a single dry-down scenario,
 293 $W(\tau)$ is equal to $W(0)$, the initial soil water availability, for any τ between 0 and T .

294 In the presence of competition for water, the dynamic feedback stomatal optimization searches for the
 295 evolutionarily stable strategy (ESS, Maynard Smith, 1974) that can guarantee a higher or equal long-
 296 term average net carbon gain rate than that of any alternative strategy of the competitors.

297 Mathematically, the ESS condition implies

$$\bar{B}_{ESS}(g_{s,ESS}(s), s_{ESS}) \geq \bar{B}_I(g_{s,I}(s), s_{ESS}) \quad (5)$$

298 where \bar{B}_{ESS} and \bar{B}_I are the long-term average net carbon gain rates of the ESS and any alternative
 299 strategy in the competition, respectively, and $g_{s,ESS}(s)$ and $g_{s,I}(s)$ are the corresponding stomata
 300 response of the ESS and any alternate strategy of an invader (subscript I). The soil moisture conditions in
 301 both cases, designated by s_{ESS} , are set by feedback from the ESS stomatal response, as the ESS was first
 302 formulated based on the idea that no competitor can benefit from switching to a strategy other than the
 303 ESS.

304 Eq. 5 can be used to find the ESS for both full and partial xylem recovery. In the case of full xylem
 305 recovery, the ESS can be found from applying Eq. 5 instantaneously, since any difference in legacy
 306 effects between strategies imposed by soil-plant feedback has been effectively eliminated by imposing

307 the same soil moisture condition, s_{ESS} , for all strategies. In the case of partial recovery, the legacy effect
308 due to permanent xylem damage remains, and the ESS can no longer be found from instantaneous
309 optimization. Rather, the ESS must first account for how the extent of xylem recovery might affect
310 stomatal conductance through reduced xylem hydraulic conductance, through a two-step process. The
311 full details of the derivation can be found in Lu *et al.* (2020).

312 **3.3. Dry-down scenarios**

313 A total of eight scenarios are explored to compare the performance of instantaneous *vs.* dynamic
314 feedback optimization with different conditions of water supply (see *Water Supply* section below),
315 competition, and permanent xylem damage (Table 3). In each scenario, both instantaneous and dynamic
316 feedback optimization with the same net carbon gain function B from Eller *et al.* (2018) (Table S1) is
317 implemented to find the optimal stomatal strategy. We examine five state variables within the plant gas
318 exchange model: relative soil water availability, transpiration rate, net carbon gain rate, stomatal
319 conductance, and permanent percentage loss of xylem hydraulic conductivity.

320 *Soil water balance*

321 The dynamics of the relative soil water availability is defined at the daily scale by

$$nZ \frac{ds}{dt} = R - E(g_s) \quad (6)$$

322 where t is the time; R is the throughfall input defined by the specific water supply condition (see below);
323 and E is the stomata-controlled transpiration rate (see Table S1 or Eq. 2.2 in Eller *et al.* (2018)). The
324 product of soil porosity n and rooting depth Z converts the relative soil moisture to a soil water depth,
325 consistent with the dimensions of the water fluxes; *i.e.*, water volumes per unit ground area and time.
326 For convenience, drainage losses below the rooting zone and lateral losses are ignored. The s can be
327 converted into soil water potential, Ψ_s , based on a soil water retention curve (Campbell, 1974):

$$\Psi_s(s) = \Psi_e s^{-q} \quad (7)$$

328 where q is the curvature parameter presumed to vary with soil texture and Ψ_e (MPa) is a reference soil
329 water potential near saturation. Then, stomatal conductance is determined according to the stomatal
330 strategy under consideration. The other three state variables (*i.e.*, transpiration rate, net carbon gain
331 rate, and permanent percentage loss of xylem hydraulic conductivity) are determined based on their

332 dependence on $\Psi_s(s)$ and stomatal conductance defined by the plant gas exchange model (see Table
333 S1).

334 *Water supply conditions*

335 Plant carbon uptake under two water supply conditions with different rainfall input are modeled: (i)
336 during a single dry-down and (ii) under stochastic rainfall. During a single dry-down, both the initial soil
337 water availability and the length of the dry-down are prescribed. There is no additional water supply till
338 the end of the dry-down. Under this condition, the water constraint defined with Eq. 4 can be simplified
339 to

$$\int_0^T E(g_s(s(t))) dt \leq nZs_0 \quad (8)$$

340 where s_0 and T are the prescribed initial relative soil water availability and dry-down duration,
341 respectively. The same single dry-down condition has also been first proposed by Cowan & Farquhar
342 (1977). In their derivations, the constraint in Eq. (8) was not formally included leaving the optimization
343 formulation with one adjustable parameter: the marginal profit that measures how much carbon is
344 gained per unit of transpired water, or “marginal carbon product of water” (Buckley & Schymanski,
345 2014).

346 The single dry-down condition lacks the key components of natural rainfall – the main source of soil
347 water supply and its variability. Cowan recognized that “Because replenishment of the reserves by
348 rainfall is irregular and unpredictable, the course plants follow in growing and using water cannot be
349 invariably successful” (Cowan, 1982). Thus, we consider also the more realistic condition where plants
350 take up carbon under stochastic rainfall, during a period equivalent to an infinite number of consecutive
351 dry downs. Under stochastic rainfall, every dry-down lasts for a random period. The soil water
352 availability at the beginning of every dry-down, expressed as water depth, is the sum of the random
353 rainfall input, and the amount of water left over from the previous dry-down.

354 To represent stochastic rainfall, one may concatenate a large number of consecutive dry downs (e.g., >
355 100). This brute-force approach may be accurate enough for any practical purpose but is too
356 computationally intensive to implement. Alternatively, we can invoke the probabilistic model of soil
357 water balance under stochastic rainfall developed by Rodriguez-Iturbe *et al.* (1999) and Laio *et al.*,
358 (2001). There, stochastic steady state conditions are assumed, and rainfall is idealized as a marked

359 Poisson process characterized by the mean rainfall event depth and rainfall frequency (the product of
 360 which is the mean rainfall rate). Given the stomatal response to the relative soil water availability, $g_s(s)$,
 361 and hence its role on the transpiration rate, the probability density function of the relative soil water
 362 availability, $p(s, g_s(s))$, can be derived from a stochastic form of the soil water differential Eq. 6 (the full
 363 derivation can be found in Rodriguez-Iturbe *et al.* (1999); a simplified form can be found in Porporato *et*
 364 *al.* (2004), Eq. 2) as

$$p(g_s(s), s) = \frac{C}{E(g_s(s))} e^{-\frac{nZ}{\alpha} s + \lambda \int_0^s \frac{nZ}{E(g_s(u))} du} \quad (9)$$

365 where C is a constant of integration defined by the normalizing condition that $p(g_s(s), s)$ must integrate
 366 to unity as s varies from 0 to 1, representing the lower and upper bounds of the relative soil water
 367 availability; α (m) is the mean depth of rainfall events; λ (day⁻¹) is mean rainfall frequency; n (-) is the soil
 368 porosity; and Z (m) is the effective plant rooting depth. Optionally, the transpiration term in this
 369 probabilistic model of soil water balance can be replaced with a more general soil water loss term that
 370 accounts for both plant transpiration and other means of soil water loss (*e.g.*, deep infiltration, surface
 371 evaporation, *etc.*). In this stochastic rainfall scenario, we can exchange the long-term average in eq 3
 372 with the ensemble average so that the long-term mean net carbon gain rate defined with Eq. 3
 373 becomes (Lu *et al.*, 2016)

$$\bar{B}(g_s(s)) = \int_0^1 B(g_s(s), s) p(g_s(s), s) ds. \quad (10)$$

374 *Implementation*

375 In the single dry-down scenario (but not in the stochastic rainfall scenario), the simulations were run in
 376 discrete time with all the state variables updated daily. In the stochastic scenario, optimal solutions are
 377 found by maximizing Eq. 10. In the search for the dynamic feedback stomatal optimization strategy
 378 without competition for water, we take a simplified approach by requiring the stomatal response to soil
 379 water potential to take on the following functional form for both single-dry down and stochastic
 380 scenarios:

$$g_s(\Psi_s) = a \cdot e^{-\left(\frac{\Psi_s}{c}\right)^b} \quad (11)$$

381 where a , b , and c are fitting parameters. This approach only approximates the theoretical solution by Lu
 382 *et al.* (2016) due to the additional numerical constraint defined with Eq. 11, but can largely reduce the

383 computation time. The three fitting parameters are optimized using Bayesian optimization (Mockus,
384 2012), an optimization algorithm for expensive-to-evaluate functions as is the case here. Care should be
385 taken to either numerically eliminate or explicitly account for the atom of probability (Rodriguez-Iturbe
386 *et al.*, 1999) that appears in the probability distribution at the lower bound of the domain of the
387 stomatal response function. In the instantaneous optimization scenario, Eq. 11 is substituted with the
388 solution from Eller *et al.* (2018) (Table S1) that relates stomatal response to plant and soil water
389 potential.

390 In the presence of competition for water, we derive the dynamic feedback stomatal optimization
391 strategy following the approach by Lu *et al.* (2020).

392 The model was written in Python and all the subsequent analyses were also conducted in Python. The
393 Bayesian optimization was implemented using the ‘bayesian-optimization’ package (Nogueira, 2014).
394 The code, including documentation, input data, and example output, can currently be found at
395 <https://github.com/feng-ecohydro/stomatal-optimization> and will be published upon manuscript
396 acceptance.

397 The model results for the single dry down case are also compared to experimental data collected in
398 Venturas *et al.* (2018) from aspen (*Populus tremuloides*) saplings subjected to a “severe drought”
399 treatment. The 4-yr-old saplings were planted in 0.8 m x 0.8 m grid and irrigated to field capacity at the
400 start of the experiment. The “severe drought” treatment, one of four treatments, received limited
401 irrigation during the experiment. The experiment lasted for more than two months, but we used data
402 only during the initial dry down before the onset of a large rainstorm that rewetted the soil. The soil,
403 atmospheric, and plant parameters adopt values published from the study. The maximum whole-plant
404 hydraulic conductance ($0.01 \text{ mol m}^{-2} \text{ s}^{-1} \text{ MPa}^{-1}$) and maximum Rubisco carboxylation rate at 25°C (120
405 $\mu\text{mol m}^{-2} \text{ s}^{-1}$) are based on the measured values at the beginning of the “severe drought” treatment, and
406 the leaf area index ($0.17 \text{ m}^2 \text{ m}^{-2}$) is set to the average value measured for saplings across the “severe
407 drought” treatment. The water potential at 50% loss in hydraulic conductivity (-1.22 MPa) is the
408 corresponding value measured at the leaves. Other parameter values used in the simulations are
409 summarized in Table 2.

410 **Table 2.** Description of symbols, definitions, values, and units of measurement. [†] and [‡] refer to values
 411 informed by Venturas *et al.* (2018) and Eller *et al.* (2018), respectively.

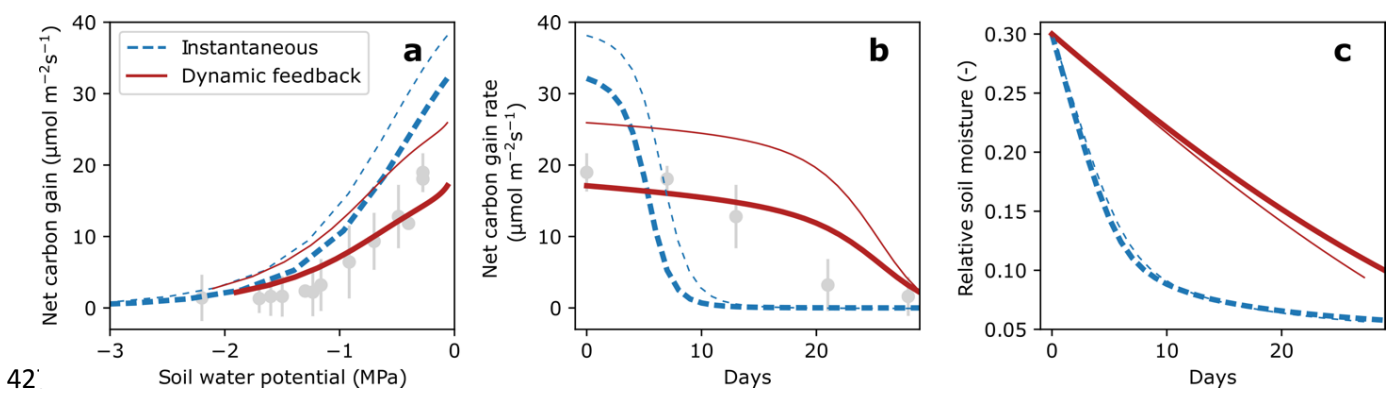
Symbol	Description	Value	Unit
Soil properties			
q	Curvature parameter for soil water retention curve	3.1	unitless
n	Soil porosity	0.38 [†]	$\text{m}^3 \text{m}^{-3}$
Z	Effective plant rooting depth	0.1	m
ψ_e	Soil water potential near saturation	-1.5e-3	MPa
Plant hydraulic & photosynthetic parameters			
a	Parameter for stomatal response to soil water potential	(0.02, 1)	$\text{mol m}^{-2} \text{s}^{-1}$
b	Parameter for stomatal response to soil water potential	(0.1, 10)	-
c	Parameter for stomatal response to soil water potential	(-1, -0.01)	MPa
LAI	Leaf area index	0.17 [†]	$\text{m}^2 \text{m}^{-2}$
k_{max}	Maximum root to leaf hydraulic conductance	0.01 [†]	$\text{mol m}^{-2} \text{s}^{-1} \text{MPa}^{-1}$
ψ_{50}	Plant water potential at 50% loss in hydraulic conductivity	-1.22 [†]	MPa
p_k	Percentage of recovered vs. unimpaired xylem conductance at a given water potential	Varies	-
$V_{cmax,25}$	Maximum Rubisco carboxylation rate at 25°C	0.00012 [†]	$\text{mol m}^{-2} \text{s}^{-1}$
ϕ	Quantum efficiency of photosynthesis	0.1 [‡]	mol mol^{-1}
ω	Leaf scattering coefficient	0.15 [‡]	-
T_{upp}, T_{low}	Upper and lower range of optimal temperature for Rubisco activity	40, 10 [‡]	°C
Environmental inputs			
α	Mean depth of rain events	Varies	m
λ	Rainfall frequency	Varies	day^{-1}
T	Dry down duration	Varies	day
T_a	Air temperature	28.7 [†]	°C
I_{PAR}	Incident photosynthetically active radiation	0.002 [†]	$\text{mol m}^{-2} \text{s}^{-1}$
D	Vapor pressure deficit	0.03 [†]	mol mol^{-1}
P_{atm}	Atmospheric pressure	90,000 [†]	Pa
C_a	Partial pressure of CO_2	40 [‡]	Pa
O_a	Partial pressure of O_2	21,000 [‡]	Pa
I	Photosynthetically active period during the day	36,000	s day^{-1}
Model state variables			
B	Net carbon gain rate	-	$\mu\text{mol m}^{-2} \text{s}^{-1}$
A	Carbon assimilation	-	$\mu\text{mol m}^{-2} \text{s}^{-1}$
θ	Carbon cost of water	-	$\mu\text{mol m}^{-2} \text{s}^{-1}$
c_i	Intercellular CO_2 pressure	-	Pa
J_c, J_l, J_e	Rubisco, light, and transport limited photosynthesis	-	$\mu\text{mol m}^{-2} \text{s}^{-1}$
K_c, K_o	Michaelis-Menten onstant for CO_2 and O_2	-	-
PLC_o	Percent loss of conductance for the undamaged xylem	-	-
E	Transpiration rate normalized by soil water storage	-	day^{-1}

g_s	Stomatal conductance to CO_2	-	$\text{mmol m}^{-2} \text{s}^{-1}$
$g_s(s)$	Stomatal response to drought	-	$\text{mmol m}^{-2} \text{s}^{-1}$
k	Plant hydraulic conductivity	-	$\text{mol m}^{-2} \text{s}^{-1} \text{MPa}^{-1}$
s	Relative soil moisture, $\in [0, 1]$	-	$\text{m}^3 \text{m}^{-3}$
W	Soil water storage ($= n Z s$)	-	m
ψ_s	Soil water potential	-	MPa
ψ_p	Plant water potential	-	MPa

412

413 **4. RESULTS**414 **4.1. Effect of soil-plant feedback on optimal stomatal conductance**

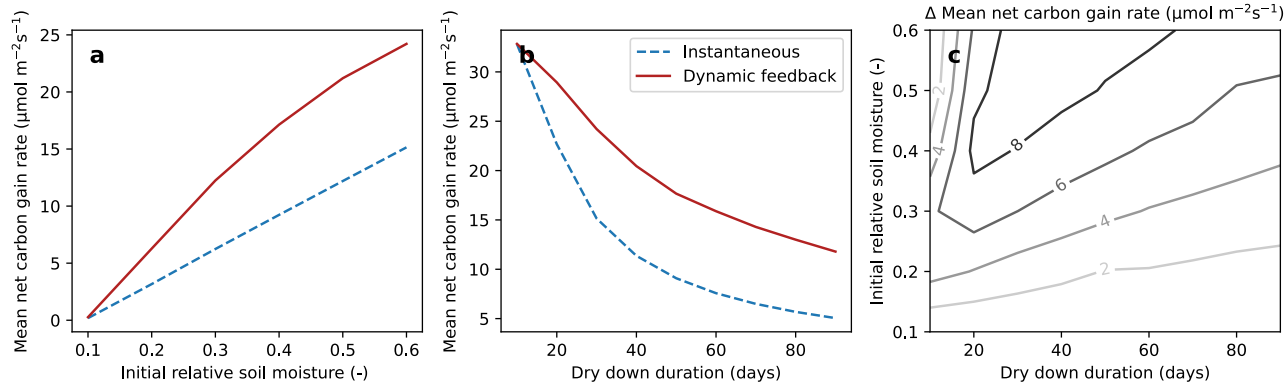
415 The results from the single dry-down scenario (Table 3, Scenario 1) show that, in the absence of
 416 competition and permanent embolism, the dynamic feedback strategy results in a much less aggressive
 417 stomatal behavior with lower stomata conductance (and thus lower net carbon gain rate) in well-
 418 watered conditions compared to the instantaneous strategy (Fig. 1a). In turn, the more aggressive
 419 stomatal strategy predicted by the instantaneous optimization results initially in a high net carbon gain
 420 rate (Fig. 1b). Because this causes faster soil water depletion (Fig. 1c), plants are forced to slow down
 421 gas exchange over time. In contrast, plants adopting the dynamic feedback strategy maintain a relatively
 422 stable gas exchange rate during the entire dry-down period. Their net carbon gain rate is lower than that
 423 of plants adopting the instantaneous strategy only at the beginning, but exceeds the latter quickly,
 424 leading to a higher total net carbon gain over the whole dry-down period. Results from both the
 425 instantaneous and dynamic feedback strategies are consistent with the range of values measured during
 426 a dry down experiment from Venturas *et al.* (2018) (Fig. 1, gray dots).



427

428 **Figure 1.** Contrasting behaviors of instantaneous and dynamic feedback strategies are shown for (a) net
 429 carbon gain rate as function of soil water potential, (b) net carbon gain rate during a single dry-down,
 430 and (c) the resulting relative soil moisture over time, in the absence of competition for water and
 431 permanent xylem embolism. Color indicates the strategy: the dynamic feedback (red solid) and

432 instantaneous (blue dashed) stomatal optimization strategies. Thick lines correspond to a scenario with
 433 $I_{PAR} = 2000 \mu\text{mol m}^{-2} \text{s}^{-1}$ and $D=0.03 \text{ mol mol}^{-1}$, and thin lines with $I_{PAR} = 1000 \mu\text{mol m}^{-2} \text{s}^{-1}$ and $D=0.015 \text{ mol mol}^{-1}$. The gray dots indicate corresponding measured values from aspen saplings in the severe
 434 drought experiment from Venturas et al. (2018), with grey lines showing the confidence intervals. The
 435 initial relative soil water availability is $s_0 = 0.3$ and the duration of the dry-down is 30 days. Soil
 436 parameters are $b = 3.1$, $\Psi_s = -0.0015 \text{ MPa}$, with porosity $n = 0.38$ and effective plant rooting depth $Z =$
 437 0.1 m. All other parameter values are as listed in Table 2.



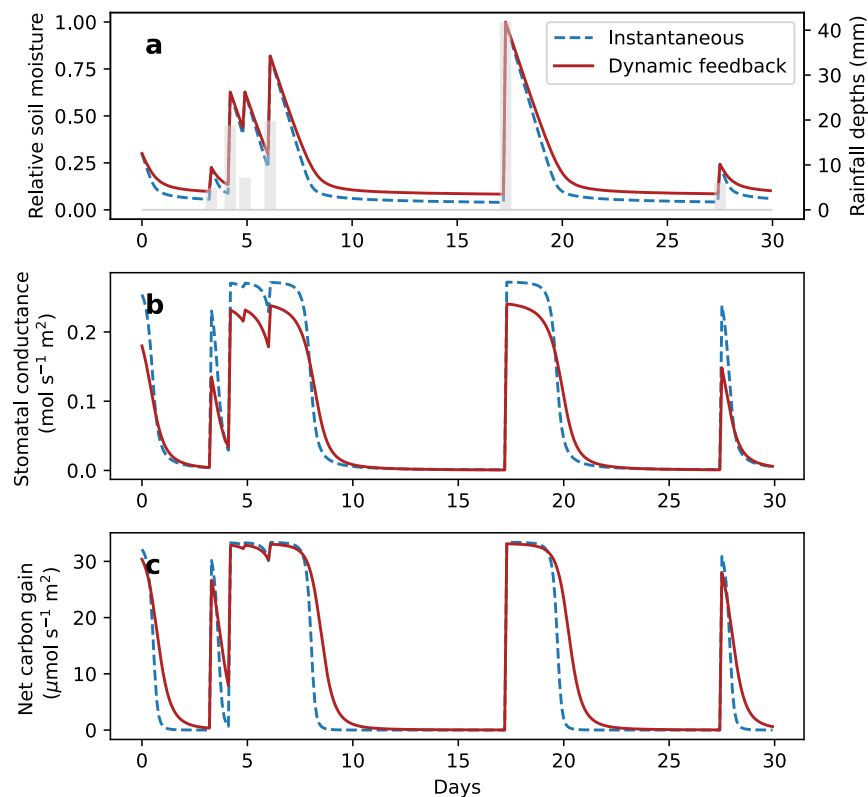
439

440 **Figure 2.** Total net carbon gain during a single dry-down for both the dynamic feedback and
 441 instantaneous strategies under varying (a) initial relative soil water availability and (b) dry down
 442 duration. The difference in net carbon gain between the dynamic feedback strategy and the
 443 instantaneous strategy are shown in (c) under a combination of dry down duration and initial soil
 444 moisture conditions. All parameter values are the same as listed in Table 2.

445 The advantage of dynamic feedback strategy over the instantaneous strategy during a single dry down
 446 varies under different dry down durations and initial soil water availabilities. The difference in the
 447 cumulative net carbon gain between the dynamic feedback strategy and the instantaneous strategy
 448 increases with increasing initial soil water availability at an intermediate dry down duration (Fig. 2c).

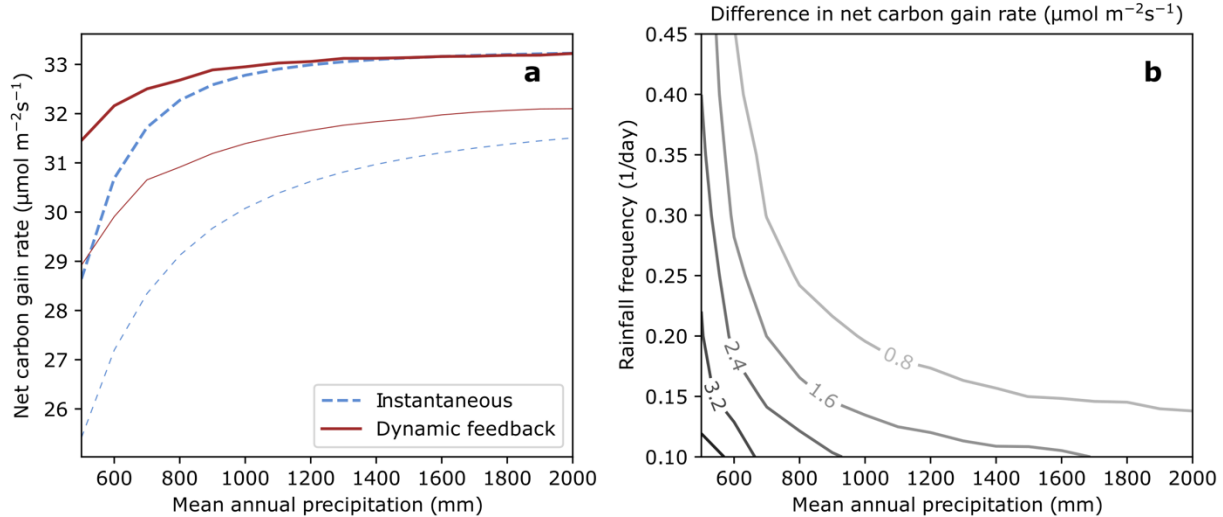
449 The same pattern between the instantaneous and dynamic feedback strategies emerges in the
 450 stochastic rainfall scenario (Table 3, Scenario 2). Here, the stochastic rainfall scenario can be
 451 represented by a consecutive series of dry downs (Fig. 3). Like the single dry down case, the
 452 instantaneous strategy tends to exhibit more aggressive water uptake that results temporarily in higher
 453 stomatal conductance and carbon gain at the beginning of each dry down (Fig. 3b, c), but more quickly
 454 depletes available soil moisture (Fig. 3a). As a result, the dynamic feedback stomatal optimization

455 strategy results in higher expected carbon gain than the instantaneous one across gradients of rainfall
 456 frequency and mean annual precipitation (Fig. 4). Also, the relative advantage of the dynamic feedback
 457 optimization strategy increases in drier climates, as the difference in net carbon gain rate between the
 458 dynamic feedback and the instantaneous strategy increases with more drought-like conditions
 459 represented by decrease in mean annual precipitation and rainfall frequency (Fig. 4b).



460

461 **Figure 3:** The relative moisture (a), stomatal conductance (b), and net carbon gain (c) of
 462 instantaneous versus dynamic feedback strategies simulated over an arbitrary 30 day period over a
 463 stochastic rainfall scenario. Frequency of rainfall is set to $\lambda = 0.15 \text{ d}^{-1}$ with mean annual precipitation of
 464 1000 mm (i.e., $\alpha = 18.3 \text{ mm}$). Light grey bars in (a) show rainfall events. All other parameters are as
 465 listed in Table 2.



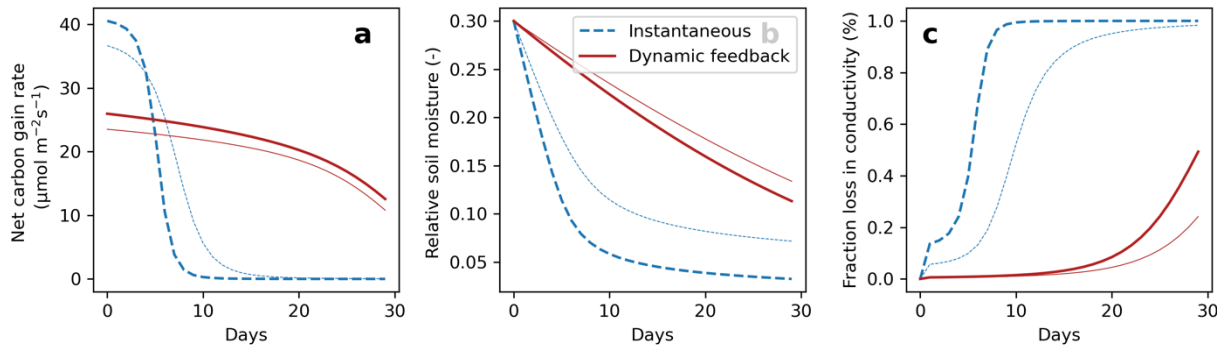
466

467 **Figure 4.** (a) The expected value of net carbon gain rates under stochastic rainfall for the instantaneous
 468 (blue dashed) and dynamic feedback (red solid) stomatal optimization strategies and (b) their difference
 469 for a range of mean annual precipitation and rainfall frequencies. These simulations are produced in the
 470 absence of competition for water and permanent xylem embolism. Line width in panel (a) indicates the
 471 rainfall frequency: $\lambda = 0.15 \text{ d}^{-1}$ (thin) and 0.30 d^{-1} (thick). All other parameters are same as listed in Table
 472 2.

473 4.2. Effect of combined soil-plant feedback and permanent xylem damage on optimal stomatal
 474 conductance

475 Considering permanent xylem embolism as an additional legacy effect on top of soil-plant feedback
 476 shows an even larger advantage of the dynamic feedback strategy over the instantaneous strategy,
 477 because the aggressive water uptake adopted by the instantaneous strategy always leads to 100% xylem
 478 embolism in the simulations. In the single dry-down scenario (Table 3, Scenario 5; Fig. 5), we consider
 479 that plants can only refill 50% of the embolized xylem. In this case, the instantaneous stomatal
 480 optimization strategy – in the absence of other physiological or phenological adjustments (e.g., leaf
 481 area) – leads to a complete loss of xylem hydraulic conductivity toward the end of the dry-down period
 482 (Fig. 5c, blue dashed lines). This potentially fatal consequence results from the lack of considering the
 483 legacy effects of permanent xylem embolism in the optimization. That is, this strategy maximizes the
 484 current net carbon gain rate without considering how resulting damage to the xylem hydraulic
 485 conductivity can reduce future carbon gain. In contrast, by accounting for the legacy effect of

486 permanent xylem damage, the dynamic feedback strategy keeps the permanent xylem damage at very
 487 low levels by restraining excessive water consumption (Fig. 5c, red solid lines). By doing so, the dynamic
 488 feedback strategy also manages to maintain higher soil water availability (Fig. 5b) and relatively high net
 489 carbon gain rate (Fig. 5a) throughout the whole dry-down period, resulting in cumulatively higher net
 490 carbon gain.



491
 492 **Figure 5.** The dynamics of net carbon gain rate (a), relative soil moisture (b), and fraction loss in
 493 conductivity (c) during a single dry-down in the absence of competition for water. Color indicates the
 494 strategy: the dynamic feedback (red) and instantaneous (blue) stomatal optimization strategies. Line
 495 width indicates different values of water potential at 50% xylem cavitation: -1 MPa (thin) and -2 MPa
 496 (thick). In this simulation, we consider plants can refill 50% of the embolized xylem. The simulation lasts
 497 for 30 days and the initial relative soil water availability is $0.3 \text{ m}^3 \text{ m}^{-3}$. All other parameter values are as
 498 listed in Table 2.

499 Because the instantaneous stomatal optimization strategy will eventually reach complete hydraulic
 500 failure when including the legacy effect imposed by (partially or completely) irreparable xylem
 501 embolism, any viable strategy will win against this strategy under competition. This is the case both
 502 during a single dry-down and under stochastic rainfall (Table 3, Scenarios 7 & 8). We have verified that
 503 the dynamic feedback stomatal optimization strategy does exist and manages to control the permanent
 504 xylem embolism with or without competition for water. In Fig. S1, we show how the expected net
 505 carbon gain rate of the dynamic feedback strategy changes with the local rainfall regime. However,
 506 when plants can always completely refill the embolized xylem, the instantaneous and dynamic feedback
 507 stomatal optimization strategies become identical under competition (Scenarios 3 & 4; Wolf *et al.*, 2016;
 508 Lu *et al.*, 2020).

509 In Table 3, we summarize the main conclusion in each of the comparisons that we have conducted. As
 510 mentioned above, the instantaneous stomatal optimization is either less productive or not viable in
 511 most comparisons with only one exception: in the presence of competition for water, the instantaneous
 512 and dynamic feedback stomatal optimization strategies are identical when plants can instantaneously
 513 and completely refill the embolized xylem (Wolf *et al.*, 2016; Lu *et al.*, 2020) (Table 3, Scenarios 3 & 4),
 514 which implies that plants can entirely eliminate the legacy effects of xylem embolism.

515 **Table 3.** A summary of the simulation results. In this table, the instantaneous and dynamic feedback
 516 stomatal optimization strategies are denoted by 'IS' and 'DS', respectively. EES refers to evolutionarily
 517 stable strategy. Lu *et al.* (2020)

No.	Permanent embolism	Competition	Dry-down scenario	Outcome	Support
1	No	No	Single dry-down	IS is less productive.	Figure 1 & 2
2			Stochastic rainfall	IS is less productive.	Figure 3 & 4
3		Yes	Single dry-down	IS and DS are identical and evolutionarily stable.	Lu <i>et al.</i> (2020)
4			Stochastic rainfall	IS and DS are identical and evolutionarily stable.	Lu <i>et al.</i> (2020)
5	Yes	No	Single dry-down	IS will reach 100% loss of hydraulic conductivity.* DS is optimal.	Figure 5
6			Stochastic rainfall	IS will reach 100% loss of hydraulic conductivity. DS is optimal.	Figure S1
7		Yes	Single dry-down	IS will reach 100% loss of hydraulic conductivity.*	Lu <i>et al.</i> (2020)
8			Stochastic rainfall	IS will reach 100% loss of hydraulic conductivity. DS is ESS.	Figure S1 Lu <i>et al.</i> (2020)

518 *During a single dry-down, the instantaneous stomatal optimization strategy may not reach 100% loss of
 519 hydraulic conductivity if the dry-down ends soon enough.

520 **5. DISCUSSION**

521 Although both the instantaneous and the dynamic feedback strategy can produce predictions that are
522 comparable to measurements (Figure 1), the sensitivity of these model results to prescribed parameters
523 (and the uncertainties associated with measuring those parameters) means that the validity of the
524 assumptions embedded in these strategies cannot be established based on existing empirical evidence
525 alone. Instead, we demonstrate the implications of those assumptions by ‘pushing’ drydowns to
526 extended periods either deterministically (in the case of a single drydown) or statistically (in the case of
527 stochastic simulations through λ). We have shown that, due to legacy effects, the instantaneous
528 strategy (maximizing instantaneous carbon gain) is neither optimal in the absence of competition nor
529 evolutionarily stable. The legacy effects that render the instantaneous strategy suboptimal are
530 represented in our analysis by soil-plant feedback and permanent xylem embolism. Each of them
531 effectively introduces a temporal tradeoff between the current and future carbon gain that encourages
532 plants to leave some water for future use when it is abundant or, equivalently, discourages excessive
533 instantaneous water consumption. In the absence of plant competition for water, these temporal
534 tradeoffs explain why maximizing instantaneous carbon gain lowers the cumulative carbon gain over
535 time. In long-term, stochastic rainfall scenarios, the advantages of the dynamic feedback strategy over
536 the instantaneous strategy increases under drought-like conditions, with lower mean annual
537 precipitation or rainfall frequency (Figure 4). In these scenarios we have set other environmental
538 variables like vapor pressure deficit and temperature to be constant because they do not impose legacy
539 effects on plants. However, the sensitivity of the results to variations in these external forcings remains
540 to be investigated.

541 For plants with shared access to water, water competition motivates plants adopt an instantaneous
542 strategy even under a limited water supply – they must use up water quickly so that the water will not
543 be used by their neighbors. Indeed, we have shown that the ESS framework effectively eliminates the
544 legacy effects of soil-plant feedback (Eq. 5). Consequently, although the instantaneous and dynamic
545 feedback stomatal optimization strategies still differ in the objective function used for stomatal
546 optimization, they arrive at the same mathematical results (Lu *et al.*, 2020) and provide the rationale for
547 the instantaneous stomatal optimization model by Wolf *et al.*, (2016). Nevertheless, competition cannot
548 eliminate the influence of other legacy effects (such as permanent xylem damage) on the optimal
549 stomatal strategy. In a scenario where the xylem is only partially (i.e., not completely) recoverable, we
550 have also shown that the instantaneous stomatal optimization strategy will inevitably lead to hydraulic
551 failure (Fig. 5) due to its aggressive water use. In contrast, the dynamic feedback stomatal optimization

552 strategy is not only viable but also evolutionarily stable. The dynamically optimal strategy is achieved by
553 controlling the soil water availability at a level that is both too high for any more conservative strategy
554 (with lower stomatal conductance and less damage in the xylem) and too low for any more aggressive
555 strategy (with higher stomatal conductance and more damage in the xylem) to be more productive (Lu
556 *et al.*, 2020).

557 In addition to the legacy effects related soil-plant feedback and permanent xylem embolism examined
558 here, there exist other legacy effects that may also play a significant role in stomatal optimization. Each
559 of these legacy effects can be associated with a different state variable that is dynamically regulated by
560 plants themselves and, in turn, affects plants' carbon gain over time. These state variables may be
561 internal to the plant, such as xylem vulnerability incurred due to water stress, or external to the plant,
562 such as the soil water availability that is subject to soil-plant feedback. Here we discuss three examples
563 of potential legacy effects due to: 1) leaf growth (constrained by plant carbon balance), 2) leaf aging
564 (constrained by RuBisCo synthesis and degradation), and 3) decline in plant hydraulic capacity due to
565 salinity (constrained by soil salt balance). By coordinating its carbon stores with water balance, plants
566 can allocate carbon toward leaf growth over time (Schymanski *et al.*, 2009). Because total leaf area also
567 influences the total transpiration rate (and thus future water availability), this allows plants to adopt a
568 dynamic feedback carbon maximization strategy that can be scaled from the leaf level (by considering
569 stomatal regulation only) to the whole-plant level (by considering stomatal regulation simultaneously
570 with leaf area; Bassiouni & Vico, 2021). By coordinating the temporal tradeoff in carbon investments
571 towards leaf growth or maintenance, plants can increase mean WUE over the course of leaf life span.
572 However, this process can be complicated by the decline in leaf photosynthetic capacity due to leaf
573 ageing (Kikuzawa, 1991; Kitajima *et al.*, 2002), which can introduce additional constraints to carbon
574 maximization. Detto & Xu (2020) shows that given the tradeoffs between total costs of RuBisCO
575 synthesis and degradation, as well as other chemical and mechanical defenses, plants can optimize the
576 control of the maximum carboxylation velocity, V_{cmax} , for the maximum cumulative photosynthesis and
577 total carbon gain over the leaf's lifespan. Finally, salinity limits water movement from the soil to the leaf
578 and thus gas exchange (Perri *et al.*, 2019; Qiu & Katul, 2020), similarly to the effect of xylem embolism.
579 Thus, we can expect stomatal regulation to also influence the plant's ambient salinity by controlling the
580 chemical equilibrium between leaf and soil salt concentrations through transpiration (which decreases
581 soil water and increases salinity).

582 All these legacy effects indicate that a modeling framework that can accommodate both the current and
583 future impacts of plants' behavior is essential to understand stomatal regulation, and more generally,
584 the whole-plant water use strategy, based on the optimality principle. However, due to its modeling
585 framework, the instantaneous stomatal optimization approach fundamentally lacks the ability to
586 incorporate these dynamical feedbacks. Competition can eliminate the legacy effects on optimal
587 stomatal response when the legacy effects are caused by variables external to the plant (such as soil
588 water availability in the case of soil-plant feedback). In this case, competition will remove any water
589 'saved' for future use. However, when the legacy effects occur internally (such as in the case of
590 permanent xylem damage), competition with neighbors will no longer compensate for the influence of
591 legacy effects on the optimal stomatal response. That is, competition will not mitigate the impacts of
592 reduced long-term hydraulic conductance caused by aggressive current water use. In those cases, the
593 more aggressive stomatal strategy resulting from the instantaneous optimization will no longer coincide
594 with the ESS.

595 **6. CONCLUSIONS**

596 In conclusion, legacy effects – the reduction in future carbon gain due to excessive current water use –
597 will always render instantaneous stomatal optimization suboptimal in terms of long-term carbon gain.
598 The presence of water competition may mitigate the impacts of some, but not all, types of legacy
599 effects. This means that the instantaneously optimal stomatal strategy is equivalent to the ESS only
600 under limited scenarios and is by no means a general result (Wolf *et al.*, 2016). Legacy effects are likely
601 ubiquitous in nature, most commonly introduced through conserved quantities like soil water supply
602 (e.g., the more water used now the less will be available for later) but also through long-term reduction
603 in water uptake capacity due to xylem damage (e.g., the more water used now the less water can be
604 acquired later). Given its success in reproducing empirical land surface fluxes (Eller *et al.*, 2020; Sabot *et*
605 *al.*, 2020; Bassiouni & Vico, 2021; Harrison *et al.*, 2021), the instantaneous stomatal optimization models
606 provide a phenomenological, 'macroscopic' representation of complex biological phenomena,
607 aggregating numerous 'microscopic' processes involved in stomatal aperture adjustments, from genetic
608 coding to physical and chemical signaling between roots and leaf. However, instantaneous stomatal
609 optimization does not offer any finality to the dynamics of g_s . So while it has been shown to capture
610 observed stomatal responses to short-term atmospheric forcing, it also has known limitations in
611 representing long-term stomatal responses, especially with respect to elevated CO₂ concentrations
612 (Katul *et al.*, 2009, 2010; Medlyn *et al.*, 2011; Buckley & Schymanski, 2014).

613 What is needed to bridge the practicality and ease of use of instantaneous models and their theoretical
614 grounding is a means for understanding the timescales over which sacrificing short-term gain for long-
615 term fitness may provide a selective advantage for plants. Such reconciliation between instantaneous
616 and time-integrated optimization has also been previously explored using the marginal carbon profit and
617 cost of water, while emphasizing the role of whole plant carbon balance (Buckley & Schymanski, 2014).
618 Here, if we compare the instantaneous solutions against the dynamic feedback solution derived using
619 the same instantaneous cost function (say, designated by θ) then we have shown here that the dynamic
620 feedback solution derived from the same cost function will always outperform the instantaneous
621 solution in the absence of competition. Then, a related and open question is this: what is the “effective”
622 cost function – denoted θ' – that mimics the long-term effects of θ ? We can surmise that θ' cannot
623 simply be a linear function of θ , as simply scaling the cost function will not yield a different optimal value
624 (but only increase or decrease the carbon gain associated with that optimal value). Therefore, the ratio
625 of θ' to θ must necessarily be a function of water availability or plant water potential. This makes
626 intuitive sense, as the ratio of θ' to θ represents a tradeoff between the current and future cost of
627 water, which should theoretically vary due to water availability and plant hydraulic state. Future work
628 can attempt to resolve the form of this exchange ratio and how it can be informed by the various
629 timescales of environmental variabilities and the degree to which plant stomatal regulation are coupled
630 to those variabilities.

631

632 **ACKNOWLEDGEMENTS**

633 X.F. and Y.L. were supported by U.S. National Science Foundation CAREER award DEB-2045610. MJ
634 acknowledges the funding from the ARC Discovery grant (DE210101654). SM has received funding from
635 the European Research Council (ERC) under the European Union’s Horizon 2020 research and innovation
636 programme (grant 101001608). GK acknowledges support from the U.S. National Science Foundation
637 (NSF-AGS-2028633, NSF-IOS-1754893) and the Department of Energy (DE-SC0022072). GV received
638 funding thanks the European Commission and Swedish Research Council for Sustainable Development
639 FORMAS (grant 2018-02787) for funding in the frame of the collaborative international consortium
640 iAquaduct financed under the 2018 Joint call of the WaterWorks2017 ERA-NET Cofund. This ERA-NET is
641 an integral part of the activities developed by the Water JPI. We also thank Stan Schymanski and an
642 anonymous reviewer for comments toward improving the manuscript.

643

644 **AUTHOR CONTRIBUTIONS**

645 Y.L. and X.F. conceptualized, designed, and performed the research; X.F. and Y.L. wrote the manuscript.
646 All other authors, listed alphabetically, contributed to refining the ideas presented in this paper,
647 interpreting the data, and editing the manuscript.

648

649 **REFERENCES**

650 **Anderegg WRL, Anderegg LDL, Berry JA, Field CB. 2014.** Loss of whole-tree hydraulic conductance
651 during severe drought and multi-year forest die-off. *Oecologia* **175**: 11–23.

652 **Anderegg WRL, Wolf A, Arango-Velez A, Choat B, Chmura DJ, Jansen S, Kolb T, Li S, Meinzer FC, Pita P, et al. 2018.** Woody plants optimise stomatal behaviour relative to hydraulic risk. *Ecology Letters* **21**:
653 968–977.

655 **Ball JT, Woodrow IE, Berry JA. 1987.** A model predicting stomatal conductance and its contribution to
656 the control of photosynthesis under different environmental conditions. In: Progress in photosynthesis
657 research. Springer, 221–224.

658 **Bassiouni M, Vico G. 2021.** Parsimony vs predictive and functional performance of three stomatal
659 optimization principles in a big-leaf framework. *New Phytologist* **231**: 586–600.

660 **Blackman CJ, Creek D, Maier C, Aspinwall MJ, Drake JE, Pfautsch S, O'grady A, Delzon S, Medlyn BE, Tissue DT. 2019.** Drought response strategies and hydraulic traits contribute to mechanistic
661 understanding of plant dry-down to hydraulic failure. *Tree Physiology* **39**: 910–924.

663 **Buckley TN. 2021.** Optimal carbon partitioning helps reconcile the apparent divergence between
664 optimal and observed canopy profiles of photosynthetic capacity. *New Phytologist* **230**: 2246–2260.

665 **Buckley TN, Miller JM, Farquhar GD. 2002.** The mathematics of linked optimisation for water and
666 nitrogen use in a canopy. *Silva Fennica* **36**: 639–669.

667 **Buckley TN, Sack L, Farquhar GD. 2017.** Optimal plant water economy. *Plant Cell and Environment* **40**:
668 881–896.

669 **Buckley TN, Schymanski SJ. 2014.** Stomatal optimisation in relation to atmospheric CO₂. *New*
670 *Phytologist* **201**: 372–377.

671 **Campbell GS. 1974.** A simple method for determining unsaturated conductivity from moisture retention
672 data. *Soil science* **117**: 311–314.

673 **Cowan IR. 1982.** Regulation of water use in relation to carbon gain in higher plants. In: *Physiological*
674 *plant ecology II*. Springer, 589–613.

675 **Cowan I. 1986.** Economics of carbon fixation in higher plants. *On the economy of plant form and*
676 *function*:

677 **Cowan IR, Farquhar GD. 1977.** Stomatal function in relation to leaf metabolism and environment.
678 *Symposia of the Society for Experimental Biology* **31**: 471–505.

679 **Cowan IR, Troughton JH. 1971.** The relative role of stomata in transpiration and assimilation. *Planta* **97**:
680 325–336.

681 **DeLucia EH, Heckathorn SA. 1989.** The effect of soil drought on water-use efficiency in a contrasting
682 Great Basin desert and Sierran montane species. *Plant, Cell & Environment* **12**: 935–940.

683 **Detto M, Xu X. 2020.** Optimal leaf life strategies determine V_c, max dynamic during ontogeny. *New*
684 *Phytologist* **228**: 361–375.

685 **Eller CB, Rowland L, Mencuccini M, Rosas T, Williams K, Harper A, Medlyn BE, Wagner Y, Klein T,**
686 **Teodoro GS, et al. 2020.** Stomatal optimization based on xylem hydraulics (SOX) improves land surface
687 model simulation of vegetation responses to climate. *New Phytologist* **226**: 1622–1637.

688 **Eller CB, Rowland L, Oliveira RS, Bittencourt PRL, Barros F V., Da Costa ACL, Meir P, Friend AD,**
689 **Mencuccini M, Sitch S, et al. 2018.** Modelling tropical forest responses to drought and El Niño with a
690 stomatal optimization model based on xylem hydraulics. *Philosophical Transactions of the Royal Society*
691 *B: Biological Sciences* **373**.

692 **Feng X, Ackerly DD, Dawson TE, Manzoni S, McLaughlin B, Skelton RP, Vico G, Weitz AP, Thompson SE.**
693 **2019.** Beyond isohydricity: The role of environmental variability in determining plant drought responses.
694 *Plant Cell and Environment* **42**: 1104–1111.

695 **Gentine P, Green JK, Guérin M, Humphrey V, Seneviratne SI, Zhang Y, Zhou S. 2019.** Coupling between
696 the terrestrial carbon and water cycles - A review. *Environmental Research Letters* **14**.

697 **Givnish TJ, Vermeij GJ. 1976.** Sizes and shapes of liane leaves. *The American Naturalist* **110**: 743–778.

698 **Hari P, Mäkelä A, Korpilahti E, Holmberg M. 1986.** Optimal control of gas exchange. *Tree Physiology* **2**:
699 169–175.

700 **Harrison SP, Cramer W, Franklin O, Prentice IC, Wang H, Brännström Å, de Boer H, Dieckmann U, Joshi**
701 **J, Keenan TF, et al. 2021.** Eco-evolutionary optimality as a means to improve vegetation and land-
702 surface models. *New Phytologist* **231**: 2125–2141.

703 **Hetherington AM, Woodward FI. 2003.** The role of stomata in sensing and driving environmental
704 change. *Nature* **424**: 901–908.

705 **Hills A, Chen ZH, Amtmann A, Blatt MR, Lew VL. 2012.** Onguard, a computational platform for
706 quantitative kinetic modeling of guard cell physiology. *Plant Physiology* **159**: 1026–1042.

707 **Hochberg U, Rockwell FE, Holbrook NM, Cochard H. 2018.** Iso/Anisohydry: A Plant–Environment
708 Interaction Rather Than a Simple Hydraulic Trait. *Trends in Plant Science* **23**: 112–120.

709 **Huang C-W, Domec J-C, Palmroth S, Pockman WT, Litvak ME, Katul GG. 2018.** Transport in a
710 coordinated soil-root-xylem-phloem leaf system. *Advances in water resources* **119**: 1–16.

711 **Hubbard RM, Ryan MG, Stiller V, Sperry JS. 2001.** Stomatal conductance and photosynthesis vary
712 linearly with plant hydraulic conductance in ponderosa pine. *Plant, Cell and Environment* **24**: 113–121.

713 **Jarvis PG. 1976.** The interpretation of the variations in leaf water potential and stomatal conductance
714 found in canopies in the field. *Philosophical Transactions of the Royal Society of London. B, Biological*

715 **Sciences** **273**: 593–610.

716 **Katul G, Manzoni S, Palmroth S, Oren R. 2010.** A stomatal optimization theory to describe the effects of atmospheric CO₂ on leaf photosynthesis and transpiration. *Annals of botany* **105**: 431–442.

717

718 **Katul GG, Oren R, Manzoni S, Higgins C, Parlange MB. 2012.** Evapotranspiration: a process driving mass transport and energy exchange in the soil-plant-atmosphere-climate system. *Reviews of Geophysics* **50**.

719

720 **Katul GG, Palmroth S, Oren R. 2009.** Leaf stomatal responses to vapour pressure deficit under current and CO₂-enriched atmosphere explained by the economics of gas exchange. *Plant, Cell and Environment* **32**: 968–979.

721

722

723 **Kikuzawa K. 1991.** A Cost-Benefit Analysis of Leaf Habit and Leaf Longevity of Trees and Their Geographical. *The American Naturalist* **138**: 1250–1263.

724

725 **Kitajima K, Mulkey SS, Samaniego M, Joseph Wright S. 2002.** Decline of photosynthetic capacity with leaf age and position in two tropical pioneer tree species. *American Journal of Botany* **89**: 1925–1932.

726

727 **Konings AG, Katul GG, Porporato A. 2010.** The rainfall-no rainfall transition in a coupled land-convective atmosphere system. *Geophysical Research Letters* **37**: 1–5.

728

729 **Konrad W, Katul G, Roth-Nebelsick A, Grein M. 2017.** A reduced order model to analytically infer atmospheric CO₂ concentration from stomatal and climate data. *Advances in Water Resources* **104**: 145–157.

730

731

732 **Konrad W, Katul G, Roth-Nebelsick A, Jensen KH. 2018.** Xylem functioning, dysfunction and repair: A physical perspective and implications for phloem transport. *Tree Physiology* **39**: 243–261.

733

734 **Laio F, Porporato A, Ridol L, Rodriguez-iturbe I. 2001.** Plants in water-controlled ecosystems: active role in hydrologic processes and response to water stress II. Probabilistic soil moisture dynamics. *Advances in Water Resources* **24**: 707–723.

735

736

737 **Lebrija-Trejos E, Pérez-García EA, Meave JA, Bongers F, Poorter L. 2010.** Functional traits and environmental filtering drive community assembly in a species-rich tropical system. *Ecology* **91**: 386–398.

738

739

740 **Leuning R. 1995.** A critical appraisal of a combined stomatal-photosynthesis model for C3 plants. *Plant, Cell & Environment* **18**: 339–355.

741

742 **Lu Y, Duursma RA, Farrior CE, Medlyn BE, Feng X. 2020.** Optimal stomatal drought response shaped by competition for water and hydraulic risk can explain plant trait covariation. *New Phytologist* **225**: 1206–1217.

743

744

745 **Lu Y, Duursma RA, Medlyn BE. 2016.** Optimal stomatal behaviour under stochastic rainfall. *Journal of Theoretical Biology* **394**: 160–171.

746

747 **Mäkelä A, Berninger F, Hari P. 1996.** Optimal control of gas exchange during drought: Theoretical analysis. *Annals of Botany* **77**: 461–468.

748

749 **Manoli G, Domec J, Novick K, Oishi AC, Noormets A, Marani M, Katul G. 2016.** Soil–plant–atmosphere conditions regulating convective cloud formation above southeastern US pine plantations. *Global change biology* **22**: 2238–2254.

750

751

752 **Manzoni S, Vico G, Palmroth S, Porporato A, Katul G. 2013.** Optimization of stomatal conductance for

753 maximum carbon gain under dynamic soil moisture. *Advances in Water Resources* **62**: 90–105.

754 **Martin-StPaul N, Delzon S, Cochard H. 2017.** Plant resistance to drought depends on timely stomatal
755 closure. *Ecology Letters* **20**: 1437–1447.

756 **Maynard Smith J. 1974.** The theory of games and the evolution of animal conflicts. *Journal of*
757 *Theoretical Biology* **47**: 209–221.

758 **Medlyn BE, Duursma RA, Eamus D, Ellsworth DS, Prentice IC, Barton CVM, Crous KY, De Angelis P,**
759 **Freeman M, Wingate L. 2011.** Reconciling the optimal and empirical approaches to modelling stomatal
760 conductance. *Global Change Biology* **17**: 2134–2144.

761 **Mockus J. 2012.** *Bayesian approach to global optimization: theory and applications.* Springer Science &
762 Business Media.

763 **Mrad A, Sevanto S, Domec J-C, Liu Y, Nakad M, Katul G. 2019.** A Dynamic Optimality Principle for Water
764 Use Strategies Explains Isohydric to Anisohydric Plant Responses to Drought. *Frontiers in Forests and*
765 *Global Change* **2**.

766 **Nogueira F. 2014.** Bayesian Optimization: Open source constrained global optimization tool for Python.
767 GitHub. See <https://github.com/fmfn/BayesianOptimization>.

768 **Palmroth S, Katul GG, Maier CA, Ward E, Manzoni S, Vico G. 2013.** On the complementary relationship
769 between marginal nitrogen and water-use efficiencies among *Pinus taeda* leaves grown under ambient
770 and CO₂-enriched environments. *Annals of Botany* **111**: 467–477.

771 **Perri S, Katul GG, Molini A. 2019.** Xylem–phloem hydraulic coupling explains multiple osmoregulatory
772 responses to salt stress. *New Phytologist* **224**: 644–662.

773 **Porporato A, Daly E, Rodriguez-iturbe I. 2004.** Soil water balance and ecosystem response to climate
774 change. *The American naturalist* **164**: 625–632.

775 **Prentice IC, Dong N, Gleason SM, Maire V, Wright IJ. 2014.** Balancing the costs of carbon gain and water
776 transport: Testing a new theoretical framework for plant functional ecology. *Ecology Letters* **17**: 82–91.

777 **Qiu R, Katul GG. 2020.** Maximizing leaf carbon gain in varying saline conditions: an optimization model
778 with dynamic mesophyll conductance. *The Plant Journal* **101**: 543–554.

779 **Rodriguez-Iturbe I, Porporato A, Ridolfi L, Isham V, Cox DR, Coxi DR. 1999.** Probabilistic modelling of
780 water balance at a point: the role of climate, soil and vegetation. *Proceedings of the Royal Society A: Mathematical, Physical and Engineering Sciences* **455**: 3789–3805.

782 **Sabot MEB, De Kauwe MG, Pitman AJ, Medlyn BE, Verhoef A, Ukkola AM, Abramowitz G. 2020.** Plant
783 profit maximization improves predictions of European forest responses to drought. *New Phytologist*
784 **226**: 1638–1655.

785 **Schymanski SJ, Sivapalan M, Roderick ML, Hutley LB, Beringer J. 2009.** An optimality-based model of
786 the dynamic feedbacks between natural vegetation and the water balance. *Water Resources Research*
787 **45**: 1–18.

788 **Siqueira M, Katul G, Porporato A. 2009.** Soil moisture feedbacks on convection triggers: The role of soil–
789 plant hydrodynamics. *Journal of Hydrometeorology* **10**: 96–112.

790 **Sperry JS, Hacke UG, Oren R, Comstock JP. 2002.** Water deficits and hydraulic limits to leaf water

791 supply. *Plant, Cell and Environment* **25**: 251–263.

792 **Sperry JS, Love DM. 2015.** What plant hydraulics can tell us about responses to climate-change
793 droughts. *New Phytologist* **207**: 14–27.

794 **Sperry JS, Venturas MD, Anderegg WRL, Mencuccini M, Mackay DS, Wang Y, Love DM. 2017a.**
795 Predicting stomatal responses to the environment from the optimization of photosynthetic gain and
796 hydraulic cost. *Plant Cell and Environment* **40**: 816–830.

797 **Sperry JS, Venturas MD, Anderegg WRL, Mencuccini M, Mackay DS, Wang Y, Love DM. 2017b.**
798 Predicting stomatal responses to the environment from the optimization of photosynthetic gain and
799 hydraulic cost. *Plant Cell and Environment* **40**: 816–830.

800 **Stocker BD, Wang H, Smith NG, Harrison SP, Keenan TF, Sandoval D, Davis T, Prentice IC. 2020.** P-
801 model v1.0: An optimality-based light use efficiency model for simulating ecosystem gross primary
802 production. *Geoscientific Model Development* **13**: 1545–1581.

803 **Venturas MD, Sperry JS, Love DM, Frehner EH, Allred MG, Wang Y, Anderegg WRL. 2018.** A stomatal
804 control model based on optimization of carbon gain versus hydraulic risk predicts aspen sapling
805 responses to drought. *New Phytologist* **220**: 836–850.

806 **Wang Y, Sperry JS, Anderegg WRL, Venturas MD, Trugman AT. 2020.** A theoretical and empirical
807 assessment of stomatal optimization modeling. *New Phytologist*: 311–325.

808 **Wolf A, Anderegg WRL, Pacala SW. 2016.** Optimal stomatal behavior with competition for water and
809 risk of hydraulic impairment. *Proceedings of the National Academy of Sciences of the United States of
810 America* **113**: E7222–E7230.

811

812